Electronic Supplementary Material (ESI) for Materials Chemistry Frontiers.

Supplementary Information

Silk fibroin microspheres as optical resonators for wide range humidity sensing and biodegradable lasers

Wey Yih Heah [a], Hiroshi Yamagishi [a], Keitaro Fujita [a], Megumi Sumitani [b], Hiroaki Yoshioka [c], Yuji Oki [c], Yohei Yamamoto*[a]

[a] Department of Materials Science and Tsukuba Research Center for Energy Materials Science (TREMS), Faculty of Pure and Applied Sciences, University of Tsukuba, 1-1-1 Tennodai, Tsukuba, Ibaraki 305-8573, Japan

[b] Division of Biotechnology, Institute of Agrobiological Sciences, National Agriculture and Food Research Organization (NARO), Owashi, Tsukuba, Ibaraki 305-8634, Japan

[c] Graduate School of Information Science and Electrical Engineering, Kyushu University, 744 Motooka, Nishi-ku, Fukuoka 819-0395, Japan

*Corresponding author. E-mail: yamamoto@ims.tsukuba.ac.jp

Materials

Bombyx mori silk cocoon was obtained from National Agriculture and Food Research Organization (NARO). Sorbitan Monooleate (Span 80), lithium bromide (LiBr, 99 %), Acid Red 52 (AR52, 98 %) and other chemicals and solvents were purchased from Tokyo Chemical Industry (TCI). Unless otherwise noted, all reagents and solvents were used as received without further purification. Ultrapure Milli-Q water was used to rinse the boiled silk cocoons and to dialyze the SF:LiBr solution. Dialysis membrane with a molecular weight cut-off (MWCO) of 12 kDa was purchased from Kenix.

Method

Dissolution of silk fibroin

An aqueous dispersion of SF was prepared according to a previous paper[1]. Silk cocoons were boiled in aqueous solution of Na_2CO_3 (0.02 M) for 30 min and then rinsed with deionized water for three times to remove the sericin coating layer from SF. The rinsed SF was dried under atmosphere at 25 °C for 1 day and then dispersed in aqueous solution of LiBr (9.3 M) at 90 °C for 1 h. The SF dispersion was dialyzed with a cellulose membrane in water for 3 days. The stock aqueous dispersion of SF (Fig. 1c) was stored at 4 °C for further usage.

Characterization

UV-vis absorption measurement was recorded on a JASCO V-570 spectrophotometer. Steady-state PL spectra were measured on a JASCO FP-6200 spectrofluorometer. μ-PL spectra were measured with a spectrometer (Lambda Vision model LV-MC3/T, grating: 300 grooves mm^{-1}), together with a 450-nm cw laser (Huanic model DD450-10-5, 10 mW) and an optical microscope (Nicon model Eclipse LD100D). μ-PL spectra with femto-second laser pumping were obtained through a spectrometer (MS7504, SOLAR TII), equipped with an optical microscope (ECLIPSE TE2000-U, Nikon) and a 800 nm fs-pulse laser (Soltice Ace, 800 nm). Scanning electron microscope (SEM) images were taken on a Hitachi model S-3700N SEM operating at 15 kV on a silicon substrate. Attenuated total reflection-Fourier transform infrared (ATR-FTIR) spectra were measured on a JASCO FT/IR-4200 Fourier transform infrared spectrometer with ATR attachment. Powder X-ray diffraction (PXRD) patterns were obtained on a RIGAKU model Miniflex600 diffractometer with a Cu$K\alpha$ radiation source (40 kV, 15

mA) at 25 °C. Bright field and fluorescence microscopy were observed with an Olympus model BX53 upright microscope.

SF microspheres dye uptake characterization

Dye concentration in SF microspheres was evaluated through absorption spectra method. 3 mg of the AR52 dyed SF microspheres were added with 3 mL of HCl (10 wt%) and heat at 90 °C for 3 h. The SF microspheres were fully disintegrated into HCl and the solution was analyzed with UV-vis measurement to obtain the absorption spectra for the solution. Besides, 3 mg of the dyed SF microspheres were added together with known amount of AR52 (0.3 mg, 3 mg, and 30 mg) into 3 mL of HCl (10 wt%) and heated at 90 °C for 3 h. The solutions were again analyzed with UV-vis measurement to obtain the absorption spectra for the solutions. The dye absorption peaks for the predetermined dye concentrations were plotted to obtain the absorption coefficient for the solutions (Fig. S1). The absorption coefficient, ε for SF:AR52 solution was 0.039 mL mg^{-1} cm^{-1}. By fitting the absorbance of the sample to the equation of Beer-Lambert law $A = \varepsilon lc$ where A is the absorbance, ε is the absorption coefficient, l is the width of the quartz cell, and c is the concentration of the dye, the concentration for the dye solution was 0.46 μg mL^{-1}. Therefore, each mg of the dyed SF microspheres contained 0.46 μg of AR52.

μ-PL measurements upon cw laser excitation

The SF microspheres were spin-casted on a Si substrate and the substrate was placed in the examination chamber beneath the glass sheet with an aperture for airflow. A 450-nm cw laser (Huanic model DD450-10-5, 10 mW) was passed through a x50 objective lens (NA = 0.9) set on an optical microscope (Nicon model Eclipse LD100D) and excited a single SF microsphere. Emission from the single microsphere was guided from the objective lens through an optical fiber with spectral resolution of 0.12 nm and a 100 μm slit to a spectrometer (Lambda Vision model LV-MC3/T, grating: 300 grooves mm^{-1}).

Humidity-dependent μ-PL measurements

The setup for humidity-dependent μ-PL spectra was set as shown in Scheme 1. The humidified air was supplied through mixture of regulated flux of dry nitrogen gas and flux of wet saturated air. The air mixture was supplied to a chamber that placing a

Bluetooth temperature and humidity sensor (Inkbird IBS-TH1, accuracy: ±2 %RH) and flowed to the examination chamber. The SF microspheres were spin-casted on a Si substrate and the substrate was placed in the examination chamber beneath the glass sheet with an aperture for airflow. A 450-nm cw laser (Huanic model DD450-10-5, 10 mW) was passed through a x50 objective lens (NA = 0.9) set on an optical microscope (Nikon model Eclipse LD100D) and excited a single SF microsphere. Emission from the single microsphere was guided from the objective lens through an optical fiber with spectral resolution of 0.12 nm and a 100 μm slit to a spectrometer (Lambda Vision model LV-MC3/T, grating: 300 grooves mm^{-1}). Humidity was regulated by adjusting the airflow of the flux of dry nitrogen gas and flux of wet saturated air through attached gas valves, controlling humidity from 24 to 95 %RH.

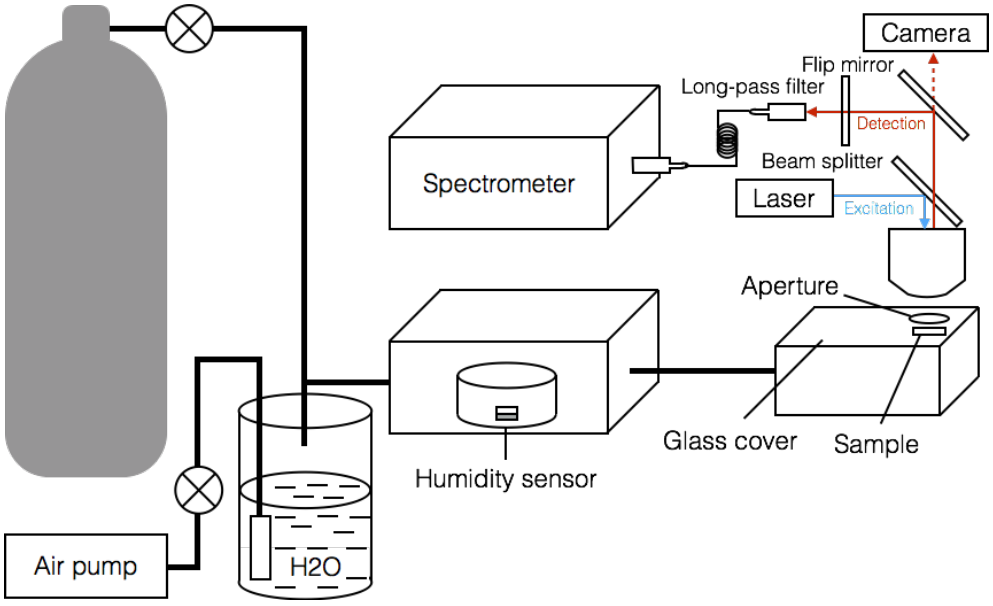

Scheme 1. Schematic diagram for the humidity-dependent μ-PL spectra setup.

μ-PL measurements upon femto-second laser pumping

The SF microspheres were also examined by optically pumping under femto-second lasing system. A pulse laser beam from laser source (Soltice Ace, λ = 800 nm) was passed through a beam splitter (Topas prime), then passed through a $2^{nd}/3^{rd}$ harmonic generator (nirUvis) and emitted 565 nm laser beam to a single SF microsphere on a quartz substrate. The emission of the excited SF microsphere was passed through a x100 objective lens on an optical microscope (ECLIPSE TE2000-U, Nikon), collimated onto the optical fiber (AFS105/125Y, Thorlabs Inc.), and pass through a 0.1 mm slit to couple to the spectrometer (MS7504, SOLAR TII).

Simulations of the WGM PL peaks

The simulations of the WGMs are conducted using Equations S1 and S2 for transverse electric (TE) and magnetic (TM) mode emissions, respectively,[2]

$$\lambda_n^E = 2\pi r(\varepsilon\mu)^{\frac{1}{2}}\left[(n+\frac{1}{2})+1.85576(n+\frac{1}{2})^{\frac{1}{3}}-\frac{1}{\varepsilon}\left(\frac{\varepsilon\mu}{\varepsilon\mu-1}\right)^{\frac{1}{2}}\right]^{-1} \quad \text{(S1)}$$

$$\lambda_n^H = 2\pi r(\varepsilon\mu)^{\frac{1}{2}}\left[(n+\frac{1}{2})+1.85576(n+\frac{1}{2})^{\frac{1}{3}}-\frac{1}{\mu}\left(\frac{\varepsilon\mu}{\varepsilon\mu-1}\right)^{\frac{1}{2}}\right]^{-1} \quad \text{(S2)}$$

where λ_n^E and λ_n^H are the wavelengths of the n-th TM and TE mode PL, respectively, ε (= η^2) is the dielectric permittivity, μ (= 1) is the magnetic permeability, and r is the sphere's radius. Here, the much higher order term was neglected. For the simulation of the emission lines, TM and TE modes were calculated using the equations S1 and S2.

Supporting Figures and Table

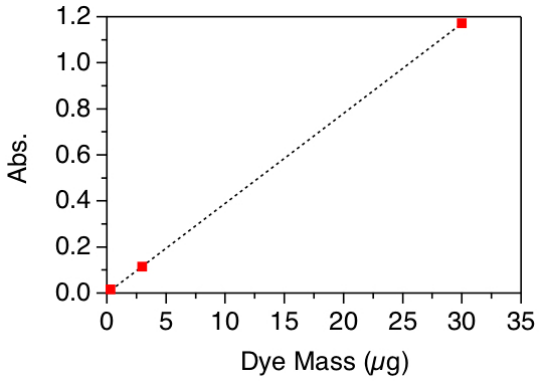

Figure S1. Plot of absorbance of aqueous solution containing SF (1 mg mL^{-1}) and AR52 at 499 nm versus dye mass.

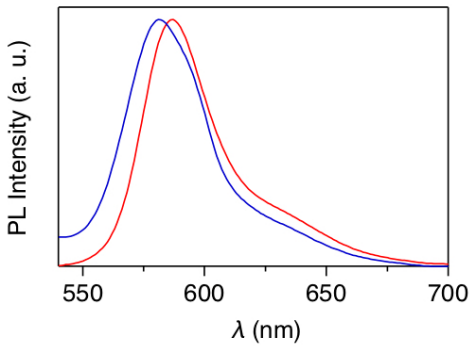

Figure S2. PL spectra of AR52 in a solution state (red) and in a solid state (microsphere, blue).

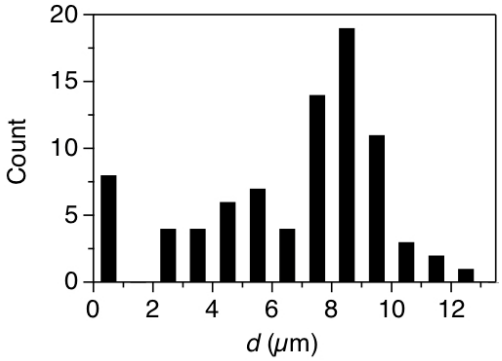

Figure S3. Histogram of the size of the SF microspheres.

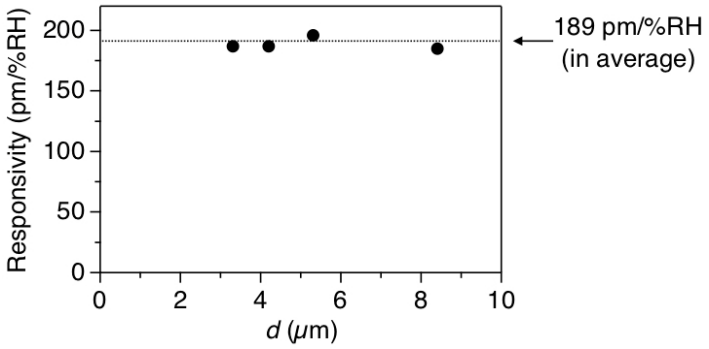

Figure S4. Plot of responsivity versus *d*.

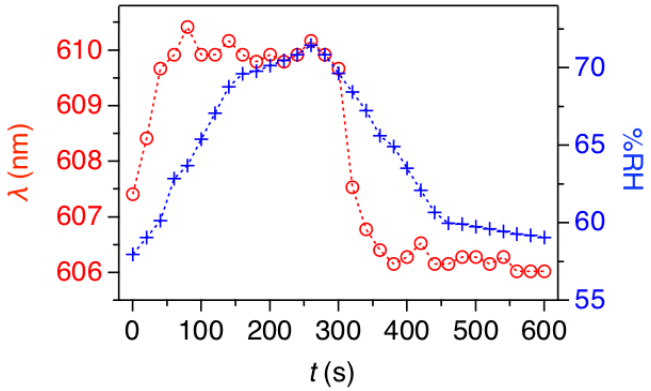

Figure S5. Plot of the WGM peak shift of SF microspheres (red) and humidity change (blue) versus time.

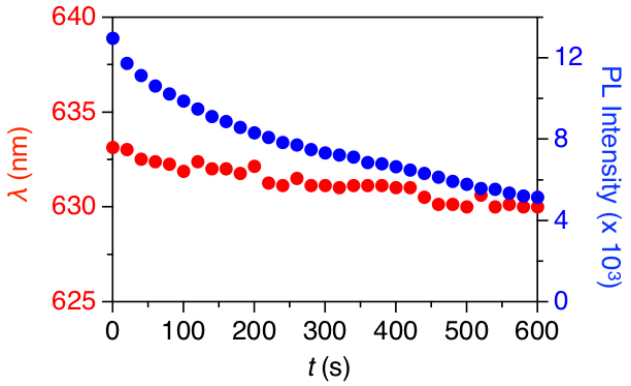

Figure S6. Plot of the WGM peak shift of the SF microspheres (red) and PL intensity (blue) versus time for continuous excitation with cw laser (λ = 450 nm).

Table S1. List of humidity sensors

Material	Technique	Sensitivity (pm/%RH)	Humidity range (%RH)	Ref.
Silk fibroin	Active resonator	187	24–95	This work
PEG-DA hydrogel	Active resonator	43.11	25–65	3
Aggregation-induced emission luminogen	Active resonator	255	34.6–70.3	4
polyethylenimine and graphene oxide	Lossy mode resonance	612	20–90	5
Agarose gel-coated	Long-period grating	114.7	25–96	6
GQD-PVA	Passive resonator	117.25	13.47–81.34	7
Spider silk	Passive resonator	389.1, 606.7	20–75	8
Silk fibroin	Reflection film	1300	7–92	9

Supporting References

1 D. N. Rockwood, R. C. Preda, T. Yücel, X. Wang, M. L. Lovett and D. L. Kaplan, *Nat. Protoc.*, 2011, **6**, 1612–1631.

2 S. Kushida, D. Braam, C. Pan, T. D. Dao, K. Tabata, K. Sugiyasu, M. Takeuchi, S. Ishii, T. Nagao, A. Lorke and Y. Yamamoto, Whispering Gallery Resonance from Self-Assembled Microspheres of Highly Fluorescent Isolated Conjugated Polymers, *Macromolecules*, 2015, **48**, 3928–3933.

3 Q.-L. Huang, H.-L. Xu, M.-T. Li, Z.-S. Hou, C. Lv, X.-P. Zhan, H.-L. Li, H. Xia, H.-Y. Wang and H.-B. Sun, *J. Light. Technol.*, 2018, **36**, 819–824.

4 A. Qiagedeer, H. Yamagishi, M. Sakamoto, H. Hasebe, F. Ishiwari, T. Fukushima and Y. Yamamoto, *Mater. Chem. Front.*, , DOI:10.1039/D0QM00722F.

5 M. Hernaez, B. Acevedo, A. G. Mayes and S. Melendi-Espina, *Sensors Actuators, B Chem.*, 2019, **286**, 408–414.

6 Y. Miao, K. Zhang, Y. Yuam, B. Liu, H. Zhang, Y. Liu and J. Yao, *Appl. Opt.*, 2013, **52**, 90–95.

7 Y. Zhao, R. jie Tong, M. Q. Chen and F. Xia, *Sensors Actuators, B Chem.*, 2019, **284**, 96–102.

8 Z. Liu, W. Liu, C. Hu, Y. Zhang, X. Yang, J. Zhang, J. Yang and L. Yuan, *Opt. Express*, 2019, **27**, 21946.

9 Q. Li, N. Qi, Y. Peng, Y. Zhang, L. Shi, X. Zhang, Y. Lai, K. Wei, I. S. Kim and K. Q. Zhang, *RSC Adv.*, 2017, **7**, 17889–17897.